

Analysis of Different Piezoelectric Materials on the Film Bulk Acoustic Wave Resonator

N. I .M. Nor^{1,2}, N. Khalid^{1,2}, H. Aris^{1,2}, M. S. Mispan³, N. Aiman Syahmi¹

¹ Faculty of Electronic Engineering Technology, Universiti Malaysia Perlis,
02600 Arau, Perlis, Malaysia

² Centre of Excellence for Micro System Technology (MiCTEC),
Universiti Malaysia Perlis, 02600 Arau, Perlis, Malaysia

³ Faculty of Electrical and Electronic Engineering Technology,
Universiti Teknikal Malaysia (UTeM), Melaka, Malaysia

ABSTRACT

The performance of film bulk acoustic wave resonators (FBAR) is greatly dependent on the choice of piezoelectric materials. Different piezoelectric materials have distinct properties that can impact the performance of FBAR. Hence, this work presents the analysis of three different piezoelectric materials which are aluminum nitride (AlN), scandium aluminum nitride (ScAlN) and zinc oxide (ZnO) on the performance of FBARs working at resonance frequencies of 6 GHz until 10 GHz. The one-dimensional (1-D) modelling is implemented to characterize the effects of these materials on the quality (Q) factor, electromechanical coupling coefficient (k^2_{eff}) and bandwidth (BW). It is determined that employing ScAlN in FBAR results in the highest Q factor, ranges from 628 to 1047 while maintaining a relatively compact area ($25 \mu\text{m} \times 25 \mu\text{m}$) and thickness (430 nm to 720 nm). However, ScAlN yields the narrowest BW, measuring 0.11 GHz at 6 GHz, as opposed to AlN and ZnO, which exhibit broader bandwidths of 0.16 GHz and 0.23 GHz, respectively.

Keywords: FBAR, AlN, ScAlN, ZnO, high Q factor

1. INTRODUCTION

Film bulk acoustic wave resonator (FBAR) has been extensively used in a wide range of applications, including wireless communication devices such as smartphones and wireless routers for filtering and frequency control, as well as sensors for various purposes, such as gas sensing and biosensing [1-6]. FBAR offers several advantages which are small size (in micrometer range), low power consumption, high frequency stability, and excellent performance in terms of insertion loss and selectivity [7]. In an FBAR, a thin film of piezoelectric material is used to generate and receive acoustic waves. Piezoelectric materials can convert electrical signals into mechanical vibrations and vice versa [8]. The bulk acoustic wave refers to the propagation of these mechanical vibrations through the thickness of the piezoelectric film. FBAR utilizes thin film technology to create a layered structure consisting of a piezoelectric material inserted in between top electrode and bottom electrode layers as illustrated in Figure 1. Acoustic waves are generated by the piezoelectric material when subjected to an electrical field due to its inherent piezoelectric properties.

* Corresponding authors: izza@unimap.edu.my

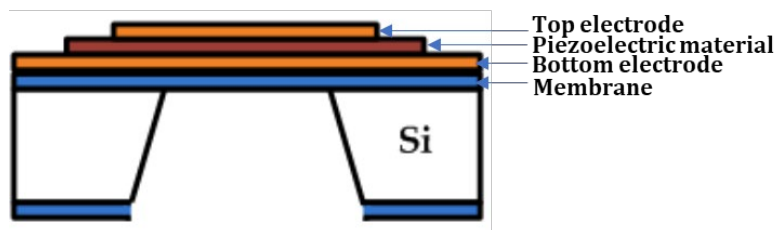


Figure 1. Cross -section of an FBAR.

Various piezoelectric materials have been widely employed in FBAR such as zinc oxide (ZnO), aluminum nitride (AlN), scandium aluminum nitride (ScAlN) and lead zirconate titanate (PZT) [2] [8-9]. PZT exhibits strong performance with 19.8% of electromechanical coupling coefficient (k^2_{eff}). However, it tends to experience high intrinsic losses when operating at high frequencies. Therefore, PZT is primarily utilized in low frequency bulk acoustic wave (BAW) devices which a high quality (Q) factor is not essential. For high frequency applications (in GHz range), ZnO, AlN and ScAlN are the commonly used piezoelectric material due to their good material properties such as high acoustic velocity and excellent dielectric constant. Table 1 summarizes the material properties of these materials.

Table 1 Properties of Piezoelectric Materials [9-10]

Properties	ZnO	AlN	ScAlN
Piezoelectric coupling coefficient, k^2_{eff} (%)	9.1	6.1	4.8
Dielectric constant, ϵ_r	9.2	9.5	10.7
Elastic modulus (GPa)	201	308	220
Density (kg/m³)	5601	3260	3601
Longitudinal Acoustic velocity (m/s)	6350	11050	8617

Most applications of FBAR require metal electrodes with low electrical resistance, high acoustic impedance, high acoustic stiffness, compatibility with standard manufacturing techniques and a suitable surface to align the piezoelectric layer. Typically, metal electrodes such as titanium (Ti), aluminum (Al), platinum (Pt) and tungsten (W) are used as electrode materials [11]. These materials have excellent electrical conductivity but poor acoustic characteristics due to low acoustic impedance. This results in low electromechanical coupling coefficient and thus restricts the achievable bandwidth. To address the issue, molybdenum (Mo) has emerged as a promising alternative due to its high acoustic impedance, low resistivity, and low density [11]. The material properties of electrode materials are summarized in Table 2.

Table 2 The Properties of Electrode Materials [11]

Properties	Al	Pt	Mo	Ti	W
Density (kg/m³)	2695	21140	10280	4480	19250
Acoustic Impedance (10⁶kg/m²s)	17.65	63.42	63.74	27.33	92.40
Phase Velocity (m/s)	6500	3260	6700	6100	5500

The electrical input impedance (Z_{in}), electromechanical coupling coefficient (k^2_{eff}) and Q factor are the key characteristics of an FBAR. The Z_{in} of an FBAR is determined by two resonant frequencies which are series resonance frequency (f_s) and parallel resonance frequency (f_p). At f_s , the electrical impedance reaches its minimum magnitude (Z_s), while at f_p the electrical impedance attains its maximum magnitude (Z_p). The k^2_{eff} holds utmost significance in FBAR design, as the

bandwidth (BW) of an FBAR is directly linked to the k_{eff}^2 of the device. Consequently, k_{eff}^2 represents one of the most significant challenges in the realm of FBAR technology. The Q factor serves as a metric for assessing the losses in a resonant circuit. In the context of FBARs, the Q factor is defined at both the series resonance frequency (Q_s) and the parallel resonance frequency (Q_p). FBARs experience various sources of losses, including acoustic leaks, losses in acoustic propagation, electrical resistivity of the electrodes, and substrate conductivity. [7]. The characteristic of an FBAR is merely dependent on the piezoelectric material and the electrode material as well as the geometrical parameters of the layers. The right choice of these materials and geometrical parameters will improve the performance of the FBAR. Thus, this work focuses on the analysis of different piezoelectric materials on the performance of FBAR working at 6 GHz until 10 GHz with a specific focus on Q factor, electromechanical coupling coefficient and bandwidth. The effect of the geometrical parameters such as thickness, width, and length on FBAR's performance is also analyzed in order to achieve optimum performance.

2. METHODOLOGY

This section focuses on the 1-D modelling of FBAR working at frequency of 6 GHz until 10 GHz by using MATLAB software. Three different piezoelectric materials are chosen as the piezoelectric layer which are AlN, ScAlN and ZnO. Firstly, the thickness of piezoelectric layer for each resonance frequency by using equation (1), where f_s is the resonance frequency of FBAR working in fundamental longitudinal mode, t is the thickness of the piezoelectric layer and v_L is acoustic velocity in longitudinal direction [12].

$$f_s = v_L / 2t \quad (1)$$

In this work, the top electrode and bottom electrode of the FBAR is molybdenum. The electrode thickness is determined by a ratio of 0.10, representing 10% of the electrode layer's thickness compared to the piezoelectric layer. This specific ratio has demonstrated superior performance, as reported in reference [12]. Then, the Mason model is applied in obtaining the electrical input impedance. The electrical input impedance, Z_{in} of a single piezoelectric layer is given in equation (2) where d is the thickness of piezoelectric layer, $k = \omega / v_L$, k_{eff}^2 is the mechanical coupling coefficient and C_0 is the static capacitance.

$$Z_{\text{in}} = \frac{1}{j\omega C_0} \left(1 - k_{\text{eff}}^2 \frac{\tan(kd/2)}{kd/2} \right) \quad (2)$$

C_0 is defined as in equation (3) where ϵ^s is the permittivity of the piezoelectric layer, d is the thickness of piezoelectric layer and A is the area. In this work, area is set to $25 \times 25 \mu\text{m}^2$, $30 \times 30 \mu\text{m}^2$ and $35 \times 35 \mu\text{m}^2$.

$$C_0 = \frac{\epsilon^s A}{d} \quad (3)$$

Meanwhile k_{eff}^2 is calculated by using equation (4), where f_s and f_p are the series resonance frequency and parallel resonance frequency respectively [12].

$$k_{\text{eff}}^2 = \left(\frac{\pi^2}{4} \right) \left(\frac{f_p - f_s}{f_p} \right) \quad (4)$$

Finally, Q factors, defined as series resonance frequency, Q_s and parallel resonance frequency Q_p can be obtained by using equation (5) where Z_{in} is the electrical input impedance and f_s and f_p are the series resonance frequency and parallel resonance frequency respectively.

$$Q_{s/p} = \frac{f_{s/p}}{2} \left[\frac{d}{df} \frac{Z_{in}}{Z_p} \right]_{f_s/f_p} \tag{5}$$

3. RESULTS AND DISCUSSION

3.1 Effect of Different Piezoelectric Materials on the Resonance Frequency

Figure 2 illustrates the correlation between the resonance frequency and the thickness for various piezoelectric materials. The findings indicate that as resonance frequencies rise, the thickness of the piezoelectric materials diminishes. This trend corroborates the idea that the acoustic path aligns proportionally with the piezoelectric film thickness, as represented in equation (1). The piezoelectric film thickness is directly associated with the acoustic path and inversely related to the resonance frequency. Additionally, it's evident that at a consistent resonance frequency, the thickness of these materials fluctuates due to differences in acoustic velocity values. AlN has shown the highest thickness at various resonance frequencies compared to ScAlN and ZnO due to its high acoustic velocity as depicted in Table 1.

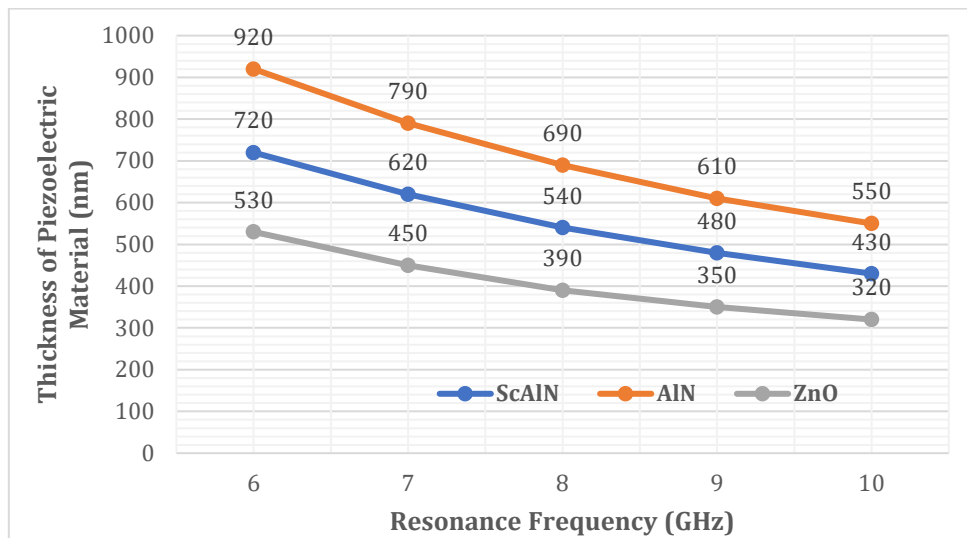


Figure 2. Effect of Different Piezoelectric Material on the Resonance Frequency.

3.2 Effect of Different Piezoelectric Materials on the Static Capacitance

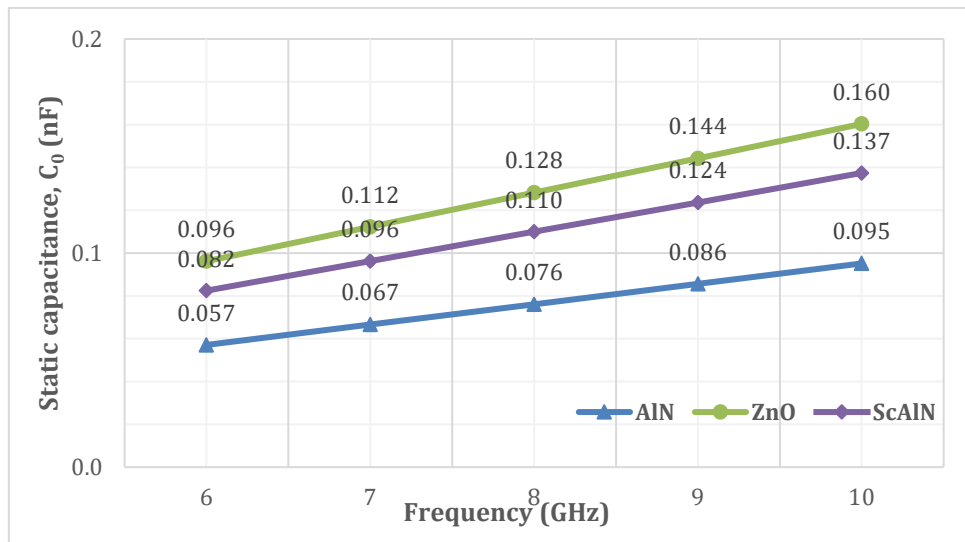


Figure 3. Effect of Different Piezoelectric Material on the Resonance Frequency.

Figure 3 shows the results of different types of piezoelectric materials and their relationship with static capacitance at resonance frequencies of 6 GHz to 10 GHz. From the figure, it is seen that AlN obtained the lowest static capacitance at the same resonance frequencies followed by ScAlN and ZnO respectively. This is due to the thickness of AlN is higher at each resonance frequency compared to ScAlN and ZnO as discussed in subsection 3.1. From the figure too, the static capacitance increases as the resonance frequency increases. This is true based on equation (3) where the static capacitance varies inversely with the thickness of the piezoelectric material.

3.3 Effect of Different Area Size on the Static Capacitance

As mentioned in section 2, three different area sizes, $25 \times 25 \mu\text{m}^2$, $30 \times 30 \mu\text{m}^2$ and $35 \times 35 \mu\text{m}^2$ are chosen to model the FBAR. Figures 4, 5, and 6 present the impact of varying area sizes of FBAR when using AlN, ZnO, and ScAlN materials, respectively. The graphs clearly indicate that the static capacitance value correlates directly with the area size of the FBARs. Thus, it can deduce that an increase in the area size leads to an augmentation in static capacitance. This relationship is further validated by equation (3). Additionally, the graphs also highlight that, at the same working frequency, the static capacitance value for FBARs using ZnO surpasses that of the other two materials. This is due to the slightly low permittivity value of ZnO, which is 9.2, while AlN and ScAlN are 9.5 and 10.7 respectively.

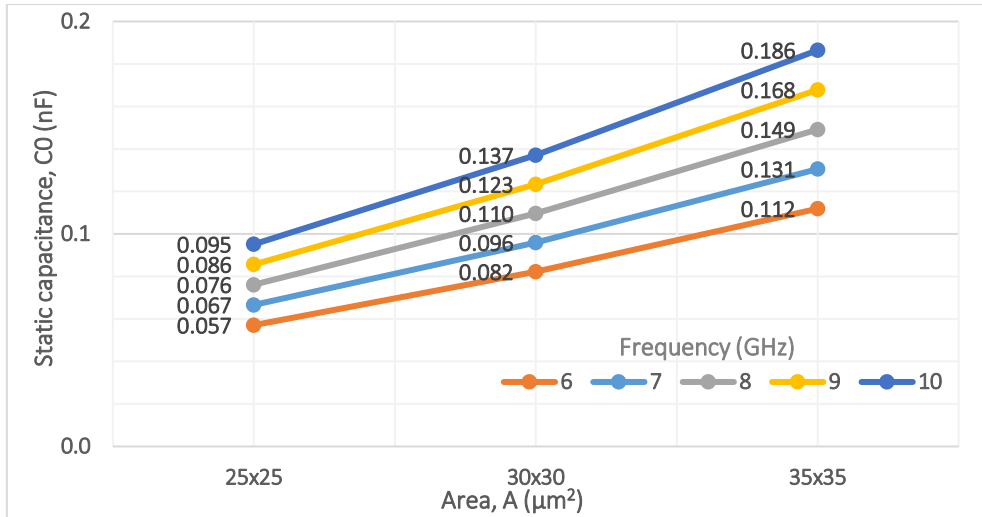


Figure 3. Effect of Area Size on the Static Capacitance using AlN.

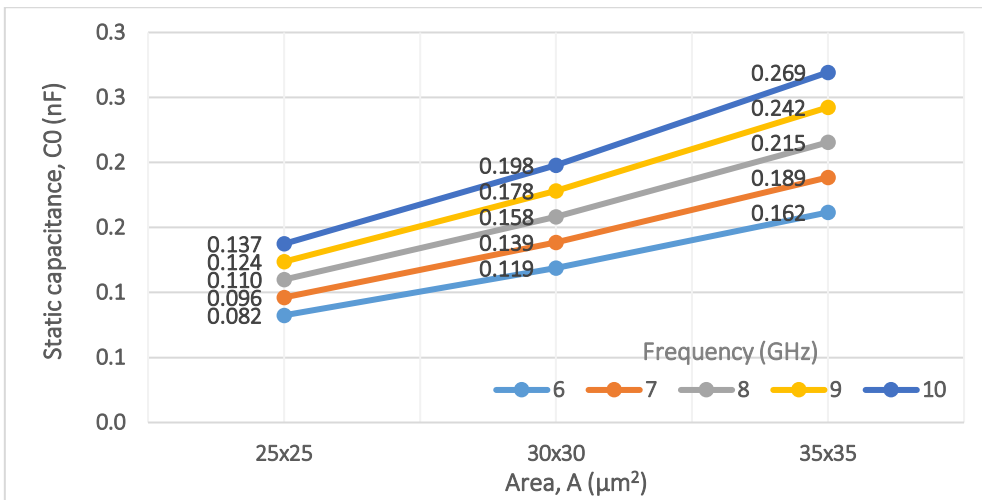


Figure 5. Effect of Area Size on the Static Capacitance using ScAlN.

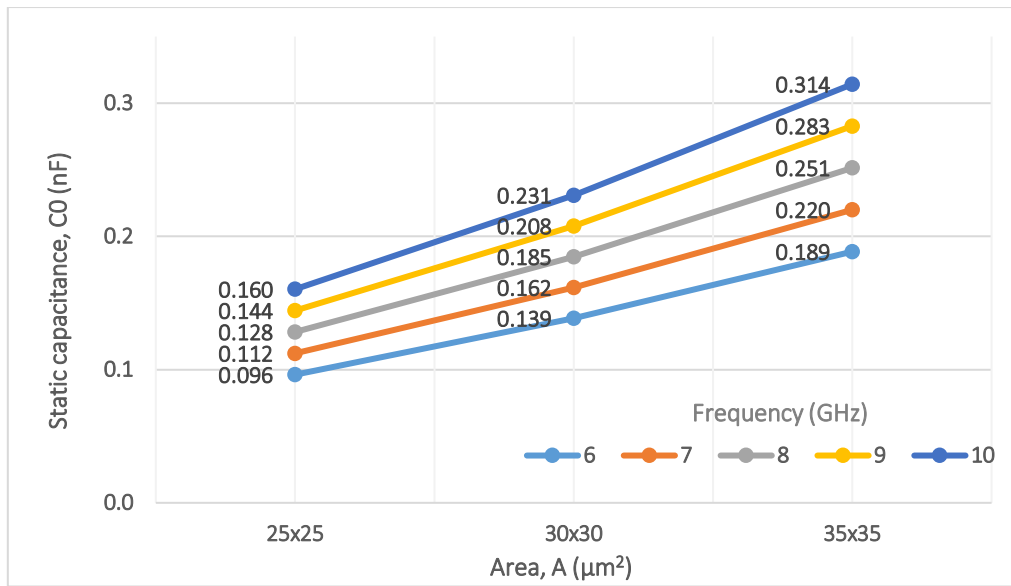


Figure 6. Effect of Area Size on the Static Capacitance using ZnO.

3.4 Effect of Different Piezoelectric Materials on the Electrical Input Impedance

Figure 7 depicts the influence of different piezoelectric materials on the electrical impedance of FBAR using AlN, ZnO and ScAlN respectively at 6 GHz. The results obtained by using equation (2). As shown in the graphs, it is seen that ZnO has the lowest Z_s and Z_p compared to AlN and ScAlN. This is mainly due to its low static capacitance value as described in subsection 3.3.

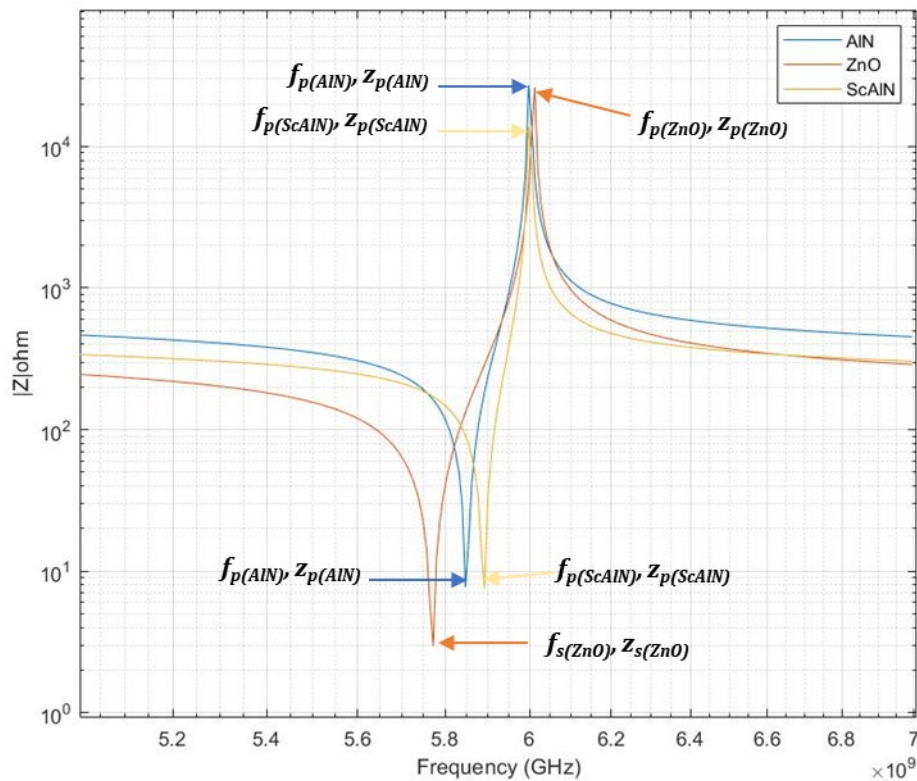


Figure 7. Effect of Different Piezoelectric Materials on the Electrical Input Impedance.

3.5 Effect of Area Size on the Electrical Input Impedance

Figure 8 shows the graphs of the influence of area size on electrical input impedance of FBAR at 6GHz. It is observed that, as the area increases, the electrical input impedance decreases. However, there is no notable change in the resonance frequency.. In terms of bandwidth (BW) which is the difference between f_s and f_p , ZnO has shown the widest bandwidth compared to AlN and ScAlN. Table 3 shows the analysis for each piezoelectric material and frequency.

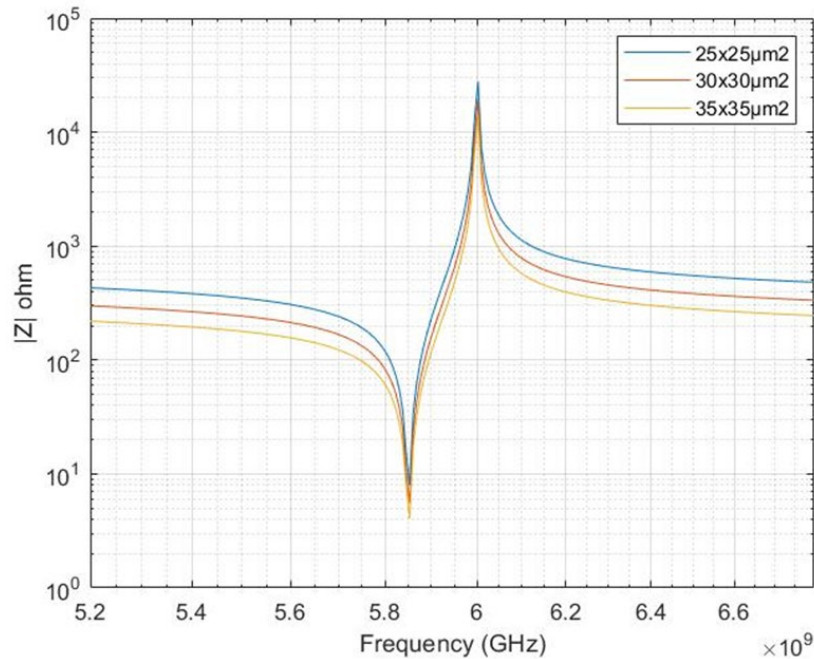


Figure 8. Effect of Different Piezoelectric Materials on the Electrical Input Impedance.

Table 3. Summary of the Effect of Different Piezoelectric Materials on the Electrical Input Impedance

Piezoelectric Material	Area (μm^2)	AlN			ScAlN			ZnO		
		Frequency (GHz)/Parameter	Z_s (Ω)	Z_p (Ω)	BW (GHz)	Z_s (Ω)	Z_p (Ω)	BW (GHz)	Z_s (Ω)	Z_p (Ω)
6	25x25	5.53	1.97e ⁴	0.158	9.34	1.14e ⁴	0.113	0.54	1.79e ⁴	0.233
	30x30	3.84	1.37e ⁴	0.158	6.48	7.93e ³	0.113	0.38	1.24e ⁴	0.233
	35x35	2.82	1.00e ⁴	0.158	4.76	5.82e ³	0.113	0.28	9.11e ³	0.233
7	25x25	4.75	2.38e ⁴	0.180	0.92	1.03e ⁴	0.143	1.36	1.37e ⁴	0.263
	30x30	3.30	1.66e ⁴	0.180	0.64	7.16e ³	0.143	0.94	9.50e ³	0.263
	35x35	2.42	1.22e ⁴	0.180	0.47	5.26e ³	0.143	0.69	6.98e ³	0.263
8	25x25	2.67	2.83e ⁴	0.203	2.71	7.22e ³	0.165	0.62	1.64e ⁴	0.308
	30x30	1.58	1.96e ⁴	0.203	1.89	5.47e ³	0.165	0.43	1.14e ⁴	0.308
	35x35	1.36	1.45e ⁴	0.203	1.39	4.02e ³	0.165	0.32	8.39e ³	0.308
9	25x25	2.06	5.26e ⁴	0.225	0.95	9.32e ³	0.180	0.74	1.98e ⁴	0.345
	30x30	1.44	3.66e ⁴	0.225	0.66	6.49e ³	0.180	0.51	1.37e ⁴	0.345
	35x35	1.05	2.68e ⁴	0.225	0.49	4.78e ³	0.180	0.38	1.01e ⁴	0.345
10	25x25	1.75	1.67e ⁴	0.225	1.83	2.32e ⁴	0.203	0.15	4.54e ⁴	0.383
	30x30	1.21	1.16e ⁴	0.225	1.27	1.60e ⁴	0.203	0.11	3.16e ⁴	0.383
	35x35	0.89	8.54e ³	0.225	0.93	1.18e ⁴	0.203	0.08	2.32e ⁴	0.383

3.6 Effect of Different Piezoelectric Materials and Area Size and on Quality Factor

Table 4 summarizes the influence of different piezoelectric materials and area sizes on the quality (Q) factor of FBAR by using equation (5). It is observed that the Q factor is increasing with the increased resonance frequencies, and it is agreeable with the equation. From the results too, it is shown that at 10 GHz, ScAlN has the highest quality (Q) factor, which is at 1026, followed by AlN then ZnO which is at 1020 and 1005 respectively. This can be attributed by the materials piezoelectric coupling coefficient (k^2_{eff}).

Table 4. Summary of the Effect of Different Piezoelectric Materials and Area Size on Q factor

Piezoelectric Material	Area (μm^2)	AlN		ScAlN		ZnO	
		Q_s	Q_p	Q_s	Q_p	Q_s	Q_p
6	25×25	613	628	617	628	604	630
	30×30	613	628	617	628	604	630
	35×35	613	628	617	628	604	630
7	25×25	714	733	718	733	705	732
	30×30	714	733	718	733	705	732
	35×35	714	733	718	733	705	732
8	25×25	817	838	820	837	805	838
	30×30	817	838	820	837	805	838
	35×35	817	838	820	837	805	838
9	25×25	918	942	924	942	906	941
	30×30	918	942	924	942	906	941
	35×35	918	942	924	942	906	941
10	25×25	1020	1046	1026	1047	1005	1046
	30×30	1020	1046	1026	1047	1005	1046
	35×35	1020	1046	1026	1047	1005	1046

4. CONCLUSION

A detailed analysis of the 1-D modelling of FBAR working at 6 GHz to 10 GHz with different design parameters has been carried out to determine the issue that influences the performance of FBAR. Molybdenum (Mo) is selected as the electrode material due to its high acoustic impedance which will improve the performance of FBAR. Furthermore, the characteristics of different piezoelectric materials, such as permittivity and longitudinal acoustic velocity, were analyzed to find the suitable combination of the piezoelectric materials with Mo. Thus, the FBAR with different piezoelectric materials with different area sizes were successfully designed to analyze the performance of FBAR. Based on the result, employing ScAlN in FBAR results in the highest Q factor, ranges from 628 to 1047 while maintaining a relatively compact area ($25 \mu\text{m} \times 25 \mu\text{m}$) and thickness (430 nm to 720 nm). However, ScAlN yields the narrowest BW, measuring 0.11 GHz at 6 GHz, as opposed to AlN and ZnO, which exhibit broader bandwidths of 0.16 GHz and 0.23 GHz, respectively. Therefore, it implies that the choice of piezoelectric material can align with the specific needs of the applications.

ACKNOWLEDGEMENTS

The authors acknowledge the Faculty of Electronic Engineering & Technology and Centre of Excellence for Micro System Technology (MiCTEC), Universiti Malaysia Perlis for the facilities and support. Special thanks to those who contributed to this project directly or indirectly.

REFERENCES

- [1] Yi Zhang, Jikui Luo, Andrew J. Flewitt, Zhiqiang Cai, Xiubo Zhao, *Biosensors and Bioelectronics*. vol **116**, issue September (2018) pp.1-15.
- [2] Z. Sabani, A. A. M. Ralib, J. Karim, N. B. Saidin & N. F. B. M. Razali, "Design and simulation of Film Bulk Acoustic Wave Resonator (FBAR) Gas Sensor Based on ZnO Thin Film," in *IEEE Regional Symposium on Micro and Nanoelectronics, Malaysia*, (2019) pp. 34-37.
- [3] Jiatai Ren *et al.*, "Research and Design of High Sensitivity FBAR Micro-mass Sensors," in *IOP Conference Series: Earth and Environmental Science, Japan*, (2021) pp. 042014.
- [4] W. Pang, M. Zhang & Q. Yang, "High Q FBAR with 21% k_{teff}² for Ultra-high Band RF Filter Applications," in *IEEE MTT-S International Microwave Workshop Series on Advanced Materials and Processes for RF and THz Applications, China*, (2022) pp. 1-1.
- [5] X. Cao, C. Wang, W. Li & Q. Cai, *IEEE Electron Device Letters*. vol **44**, issue 4 (2023) pp. 682-685.
- [6] Y. Zou *et al.*, *Journal of Microelectromechanical Systems*. vol **32**, issue 3 (2023) pp. 263-270.
- [7] N. I. M. Nor, "Wide Bandwidth Film Bulk Acoustic Wave Resonator for Ku-band Filters," in *PhD Thesis, La Trobe University, Australia*, (2013) pp. 20-49.
- [8] Pillai, G., & Li, S.-S., *IEEE Sensors Journal*. vol **21**, issue 11 (2021) pp.12589–12605.
- [9] Liu Y, Cai Y, Zhang Y, Tovstopyat A, Liu S, Sun C. *Micromachines*. vol **11**, issue 7 (2020) pp.630.
- [10] Konno, A., Kadota, M., Kushibiki, J., Ohashi, Y., Esashi, M., Yamamoto, Y., & Tanaka, S., "Determination of full material constants of ScAlN thin film from bulk and leaky Lamb waves in MEMS-based samples" in *IEEE International Ultrasonics Symposium, USA*, (2014) pp.273–276.
- [11] Y. Q. Fu, J. K. Luo, N. T. Nguyen, A. J. Walton, A. J. Flewitt, X. T. Zu, Y. Li, G. McHale, A. Matthews, E. Iborra, H. Du, W. I. Milne, *Progress in Materials Science*. vol **89**, issue August (2017) pp.31-91.
- [12] Nor N. I. M., Khalid N., Hashim N. A., Kasjoo S., Sauli Z., Lang L. H., Qi C.S., *International Journal of Nanoelectronics and Material.*, vol **14**, Special Issue InCAPE (2020) pp. 79 – 85.